18. It should be noted that this correlation is not based on matching the climate proxies themselves.
19. E. Bard, *Nature* **382**, 241 (1996).
20. H. Kitagawa, J. van der Plicht, *Science* **279**, 1187 (1998).
21. B. Kromer *et al*., *Radiocarbon* **38**, 607 (1996).
22. K. A. Hughen, J. R. Southon, S. J. Lehman, J. T. Overpeck, *Science* **290**, 1951 (2000).
23. The most conservative correlation error between the Lake Suigetsu and Cariaco records is <200 years, but the actual error is likely to be <100 years. This error is not cumulative with that associated with the anchoring of the Suigetsu and Cariaco floating chronologies to the German dendrochronology series.
24. M. Tsukada, in *Vegetation History*, B. Huntley, T. Webb III, Eds. (Kluwer Academic, Dordrecht, Netherlands, 1988), pp. 459–518.
25. Pollen spectra from the topmost horizon from each core are also included in the data set, except where the depth below the sediment surface exceeds 50 cm. Those samples are likely to reflect vegetation of a few centuries ago, predating the severe deforestation of the industrialization period.
26. K. Gotanda *et al*., *Quat. Sci. Rev*. **21**, 647 (2002).
27. Lake Suigetsu and Lake Mikata are connected by a narrow strait, the only water inlet of Lake Suigetsu. Hence, both lakes have practically identical pollen catchment areas.
28. T. Nakagawa, P. E. Tarasov, K. Nishida, K. Gotanda, Y. Yasuda, *Quat. Sci. Rev*. **21**, 2099 (2002).
29. The average interval between samples, based on varve counting, is typically 25.2 years for the pre-Holocene and 18.6 years for the Holocene.
30. More than 300 arboreal pollen grains were counted per sample; percentage values were calculated using the sum of the 32 arboreal taxa previously determined to be suitable for biome reconstruction (*26*).
31. J. Guiot, *Palaeogeogr. Palaeoclimatol. Palaeoecol*. **80**, 49 (1990).
32. We thank J. J. Lowe for improving the English and for general advice and C. Inoue for assistance with laboratory work. Supported by a Grant-in-Aid for Center of Excellence Research (grant number 09CE1001 to Y.Y.) from the Ministry of Education, Culture, Sports, Science and Technology (Japan).

9 September 2002; accepted 17 December 2002

The Perfect Ocean for Drought

Martin Hoerling[1]* and Arun Kumar[2]

The 1998–2002 droughts spanning the United States, southern Europe, and Southwest Asia were linked through a common oceanic influence. Cold sea surface temperatures (SSTs) in the eastern tropical Pacific and warm SSTs in the western tropical Pacific and Indian oceans were remarkably persistent during this period. Climate models show that the climate signals forced separately by these regions acted synergistically, each contributing to widespread mid-latitude drying: an ideal scenario for spatially expansive, synchronized drought. The warmth of the Indian and west Pacific oceans was unprecedented and consistent with greenhouse gas forcing. Some implications are drawn for future drought.

Prolonged below-normal precipitation and above-normal temperatures led to drought during 1998–2002 over an extensive swath of the Northern Hemisphere mid-latitudes spanning the United States, the Mediterranean, southern Europe, and Southwest and Central Asia (*1*–*3*). As little as 50% of the climatological annual average precipitation fell in these regions during the 4-year period (Fig. 1, right panel), and the bulk of that deficit resulted from a failure of the normally abundant winter and spring rains. Moisture deficits were aggravated by increased moisture demand resulting from above-normal temperatures (Fig. 1, left panel) that reached record proportions in recent years over the land areas (*3*).

Did these regional droughts share a common influence? Were slow, external forcings responsible for sustaining drought conditions simultaneously across a wide expanse of the mid-latitudes? In light of scientific evidence that the warming during the late 20th century is consistent with the expected impact of increased greenhouse gases (*4*), it is plausible that human activities played a role to the extent that the unusually warm land temperatures evident in Fig. 1 contributed to desiccation. Yet the recent droughts were most remarkable for their large deficits in precipitation, and the results of climate-change research on the response of precipitation are more ambivalent. It is considered likely that increased greenhouse gases intensified the global hydrologic cycle in the latter half of the 20th century, a process that would render some regions wetter and others drier and would also increase the likelihood for extreme precipitation (*4*, *5*). What is not well known, and what limits an attempt to attribute the current drought to global warming, is how precipitation would respond regionally.

Anomalous states of tropical sea surface temperatures (SSTs) also are known to cause planetary-scale climate disruptions (*6*). El Niño–Southern Oscillation (ENSO) strongly influences patterns of seasonal precipitation in the tropics and portions of the mid-latitudes (*7*–*9*). As will be shown, the 1998–2002 period of drought coincided with a protracted cold phase of ENSO (La Niña). Studies of La Niña impacts show a drying over the southern United States during boreal winter and spring, and a drying over western Europe and the Mediterranean throughout the seasonal cycle (*8*–*10*). It has also been speculated that the cold SSTs in the east Pacific, together with above-normal SSTs in the Indian and west Pacific during this period, may have caused the Asian drought (*11*). These investigations support the hypothesis that the regional droughts during 1998–

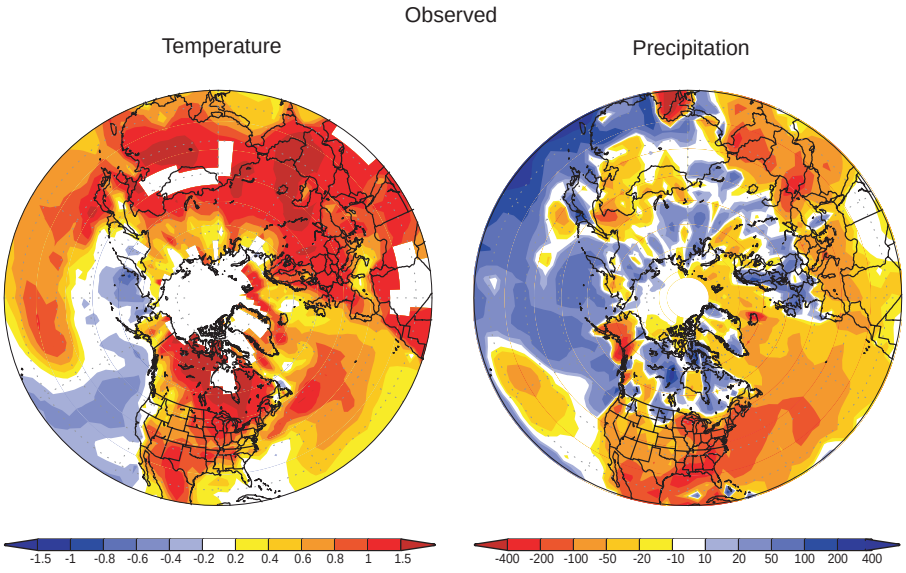

Fig. 1. Observed, annually averaged surface temperature (**left**) and precipitation (**right**) anomalies during the 4-year period June 1998–May 2002. Temperature departures are degrees Celsius computed relative to a 1971–2000 climatology. Precipitation departures are mm/year computed relative to a 1979–1995 climatology. The largest warm and dry departures are highlighted in red.

[1]Climate Diagnostics Center, National Oceanic and Atmospheric Administration (NOAA), Boulder, CO 80305, USA. [2]Climate Prediction Center, NOAA, Camp Springs, MD 20746, USA.

*To whom correspondence should be addressed. E-mail: Martin.P.Hoerling@noaa.gov

2002 may have resulted from oceanic sources related to ENSO.

Of course, the atmosphere alone, independent of oceanic or other external forcing, can cause synchronous covariability of climates that circumscribe the globe (*12*, *13*). These zonally symmetric, annular-like modes are associated with meridional displacements of the westerly jets and their storm tracks at all longitudes, which can create a situation conducive for drying of the lower mid-latitudes. Dynamical studies (*13*) indicate the existence of regional centers of action within these annular mode states over Southwest Asia, the North Pacific, the eastern United States, and Europe. Such a circulation pattern was indeed observed during 1998–2002. However, the atmosphere carries little memory beyond 1 month, and the question remains as to the cause for the multiyear persistence of an atmospheric circulation pattern that was closely tied to, if not the immediate cause of, the droughts.

Analysis of oceanic behavior during 1998–2002 reveals a remarkable persistence of tropical SST anomalies that may have provided the necessary steady forcing of the atmosphere. Figure 2 shows SST anomaly time series averaged spatially over the Indian and west Pacific (90°E–150°E, 15°N–15°S) and the tropical east Pacific (150°W–90°W, 5°N–5°S), respectively. Warmth over the Indo-west Pacific was uninterrupted during the period, and the cold La Niña conditions that developed in June 1998 lingered through winter 2002. The cold SST anomalies show pronounced seasonality, with the amplitudes peaking in early winter and weakening in late spring. Figure 2 (top) also displays the June 1998–May 2002 4-year–averaged SST anomaly pattern, standardized by the variability of 4-year averages (*14*). The 4-year–averaged anomalies exceeded −3 standardized departures in the east Pacific and +4 departures over the warm pool, confirming the extreme, sustained aspect of the oceanic forcing.

Atmospheric general circulation models (GCMs) forced by the monthly varying global SST anomalies of this period provide strong evidence that the observed pattern of Northern Hemisphere precipitation deficits and warmth over the continents was consistent with a response to oceanic forcing. The results (Fig. 3) are of a multimodel average calculated from three different GCMs (*15*), each run in an ensemble mode, yielding a grand 50-member average (*16*). The simulations capture the drying over the United States, southern Europe, and Southwest and Central Asia. Despite the model results having been derived from a 50-run average, the amplitude of the observed (single realization) precipitation deficit is recovered by the ensemble mean. This suggests that the observed drying was strongly oceanic controlled, an interpretation also supported by a reproducibility of such drying among individual members of the models' ensembles as well as among the three separate models individually (*17*). The amplitude of that drying, however, varies from run to run, with some experiments exceeding the observed precipitation deficits while others are not as dry as observed (*17*).

The immediate cause for sustained drought was an equally persistent tropospheric circulation pattern, and Fig. 4 (left) shows the 4-year–averaged 200-mbar height anomalies. An almost uninterrupted zonal belt of high pressure wrapped the middle latitudes. The GCMs simulate this feature (Fig. 4, right) and furthermore reproduce the local maxima in high pressure over the North Pacific, the central United States, and Asia. The spatial correlation of the observed and GCM-simulated 200-mbar height anomalies for the Northern Hemisphere poleward of 20°N is 0.7. The drying in the lower mid-latitudes is the direct result of this anomalous pressure pattern, and the atmospheric models confirm it to have been forced by the oceans. The GCM results are much less realistic in reproducing the wavy pattern of height anomalies

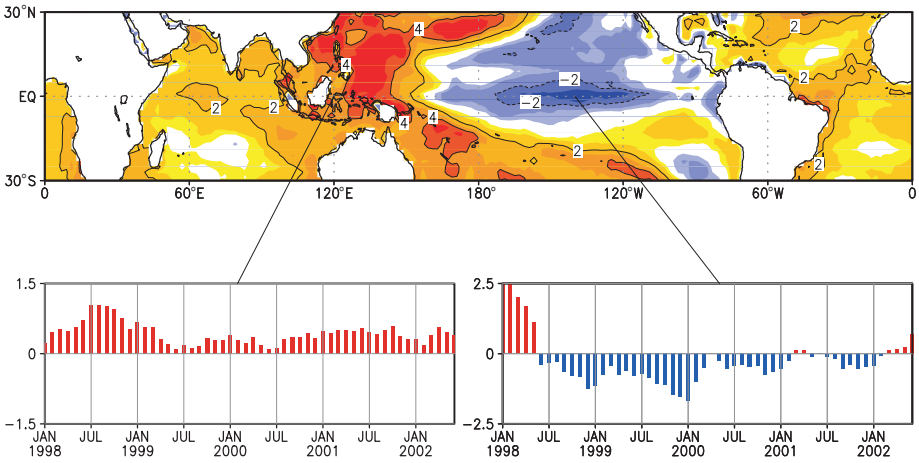

Fig. 2. Observed, standardized 4-year–averaged SST anomalies for June 1998–May 2002 (**top**). The normalization is by the standard deviation of 4-year–averaged SST variability during 1948–1998. Inserts show the monthly time series of SST anomalies during January 1998–May 2002 for the climatological warm pool region of the tropical Indian and west Pacific (90°E–150°E, 15°N–15°S) (**left**) and the climatological cold tongue region of the equatorial east Pacific (150° W–90° W, 5° N–5° S) (**right**). Anomalies are in degrees Celsius computed relative to a 1971–2000 climatology.

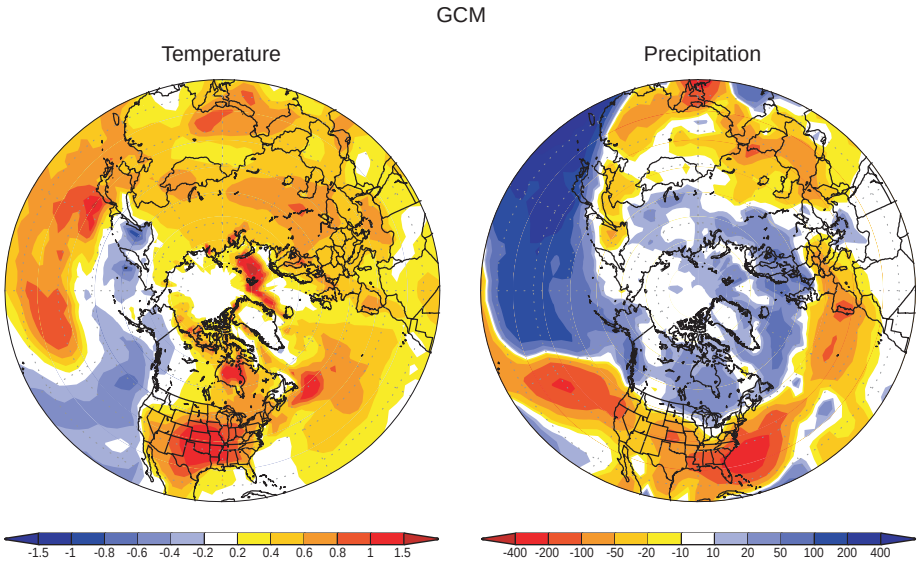

Fig. 3. Simulated, annually averaged surface temperature (**left**) and precipitation (**right**) anomalies for the 4-year period June 1998–May 2002. Results are based on atmospheric GSMs forced with the observed, monthly varying SST and sea ice anomalies of the period. Three different models, each run in ensemble mode, were combined to yield a 50-member grand ensemble. Temperature departures are degrees Celsius computed relative to the models' 1971–2000 climatology. Precipitation departures are mm/year computed relative to the models' 1971–2000 climatology. The largest warm and dry departures are highlighted in red.

over polar latitudes; thus, factors other than the oceans may have been responsible for the observed atmospheric circulation anomalies at the high latitudes, although model biases may also be responsible.

The likelihood of a tropical origin for the midlatitude circulation pattern is suggested by the fact that both observed and simulated atmospheric anomalies exhibit strong symmetry with respect to the equator, such that the Southern Hemisphere anomalies during the period mirror those in the Northern Hemisphere (*17*). Three additional experiments were performed to isolate the role of the tropical SSTs. In one, the spatial pattern and amplitude of the June 1998–May 2002 4-year–averaged SST anomaly between 30°N and 30°S (Fig. 5, top) was specified as a seasonally invariant, fixed forcing. In the second, only the anomalously warm SSTs of this field were specified, and in the third only the anomalously cold SSTs were specified (*18*). Outside these regions, climatological SSTs were specified. A 20-member ensemble was performed for each scenario, and the annually averaged Northern Hemisphere precipitation response of each ensemble is shown in Fig. 5 (lower panels). Much of the pattern of midlatitude drying seen in observations and in the GCM ensembles forced by realistic monthly varying global SST is reproduced with this simplification of the tropical SST forcing (Fig. 5, left), as is the pattern of the 200-mbar height anomalies (*18, 19*). The anomalously warm and cold portions of the tropical SSTs (Fig. 5, middle and right) each influence the drying signal over the United States and portions of the Mediterranean and Asia, but reproduction of the full drying pattern appears to require the constructive action of both. This synergy of impacts provides an addition-

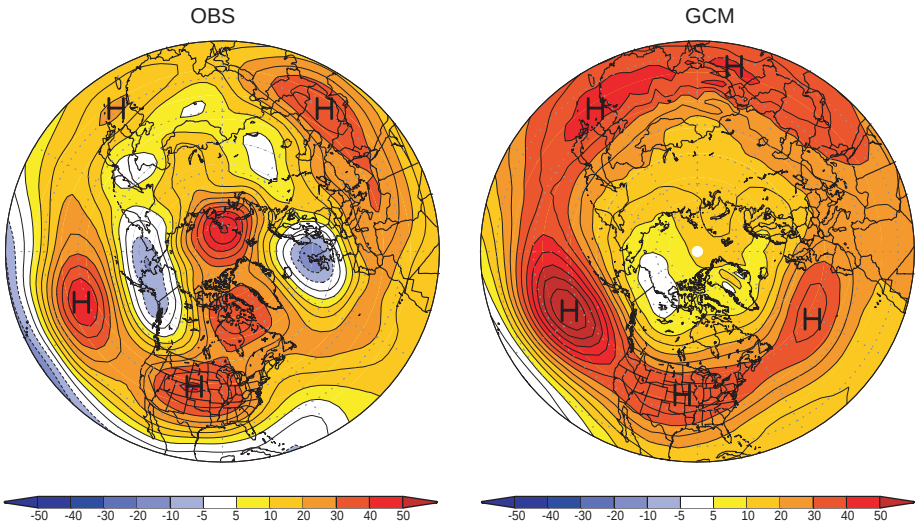

Fig. 4. Observed (**left**) and simulated (**right**) annually averaged 200-mbar height anomalies during the 4-year period June 1998–May 2002. The atmospheric GCMs were forced with the observed, monthly varying SST and sea ice anomalies of the period. Three different models, each run in ensemble mode, were combined to yield a 50-member grand ensemble. Departures are meters computed relative to the observed and model-simulated 1971–2000 climatologies, respectively. Centers of maximum positive height anomalies in the mid-latitudes are denoted by H.

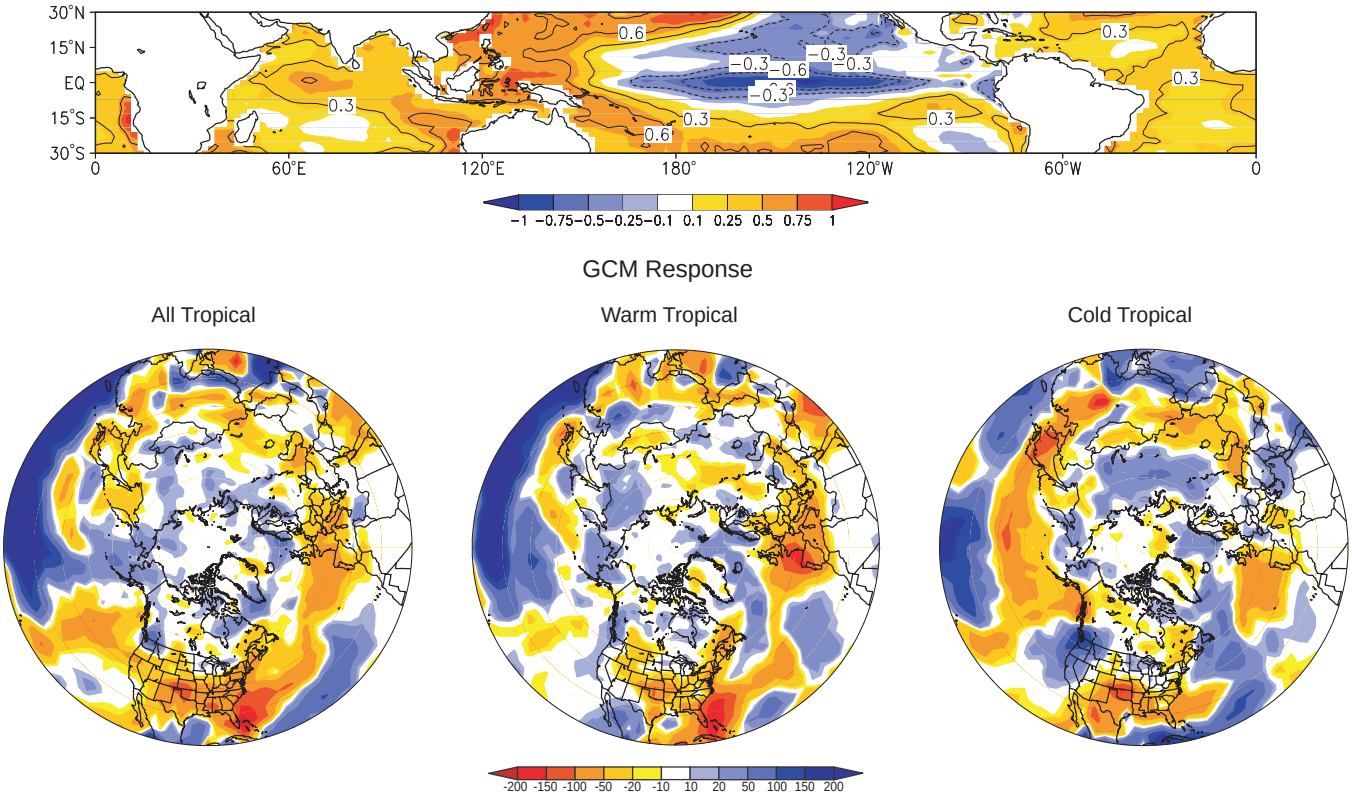

Fig. 5. Observed, 4-year–averaged sea surface temperature anomalies for June 1998–May 2002 used as the seasonally fixed forcing of the atmospheric GCM (**top**). The annually averaged precipitation response of the GCM to the entire tropical pattern of the SST forcing (**left**), warm SST subset of the SST forcing (**middle**), and cold SST subset of the SST forcing (**right**). Precipitation departures are mm/year computed relative to a control version of the GCM that takes into account only climatological SSTs. The largest dry departures are highlighted in red. SST anomalies in the top panel are degrees Celsius.

al clue as to why the tropical oceans exerted such strong control over atmospheric events leading to the droughts of 1998–2002. Together with the unusual persistence of the tropical-wide SST anomaly pattern itself, the modeling results offer compelling evidence that the widespread mid-latitude drought was strongly determined by the tropical oceans. It is thus more than figurative, although not definitive, to claim that this ocean was "perfect" for drought insofar as it satisfied many of the requirements for severe, sustained precipitation deficits and temperature increases.

To what, then, can the tropical SST anomalies of 1998–2002 be attributed? ENSO is a naturally occurring fluctuation of the coupled ocean-atmosphere system (*20*), and climate proxy records (for instance, ice cores, tree rings, and corals) suggest that this phenomenon has occurred for millennia (*21*). Even the persistence of the cold SST conditions during the 4-year period, although unusual, was not unprecedented (*10*, *22*). This and other evidence indicates that the recent statistics of ENSO have not changed detectably beyond the range of natural variability (*23, 24*). On the other hand, the warmth of the tropical Indian Ocean and the west Pacific Ocean was unsurpassed during the 20th century, being embedded within a multidecade warming trend. Climate attribution studies find that this warming (roughly 1°C since 1950) is beyond that expected of natural variability and is partly due to the ocean's response to increased greenhouse gases (*25, 26*). The state of the tropical ocean during 1998–2002 thus combined a naturally occurring, interannual cooling of the eastern Pacific with a lower frequency, possibly inexorable, warming of the Indian and west Pacific oceans. The resultant exaggeration of zonal contrast in SST did not occur during the prior, protracted La Niña periods of the 20th century, providing a unique oceanic condition during 1998–2002. It is an open question whether such tropical oceanic forcings will become more prevalent during the 21st century. Because of deficiencies in coupled ocean-atmosphere models, little confidence exists with regard to projections of the future statistics of ENSO (such as its duration and amplitude) or of the regional pattern of mean tropical SST change itself. The atmospheric modeling results of 1998–2002 suggest an increased risk for severe and synchronized drying of the mid-latitudes if the tropical mean SSTs or their interannual variability increase the ocean's west-east contrast over the equatorial Pacific.

References and Notes

1. G. Bell *et al.*, *Bull. Am. Meteorol. Soc.* **81**, 1328 (2000).
2. J. Lawrimore *et al.*, *Bull. Am. Meteorol. Soc.* **82**, 1304 (2001).
3. A. M. Waple *et al.*, *Bull. Am. Meteorol. Soc.* **83**, 938 (2002).
4. IPCC, *Climate Change 2001: The Scientific Basis: Summary for Policy Makers and Technical Summary of the Working Group I Report* (Cambridge Univ. Press, Cambridge, 2001).
5. IPCC, *Climate Change 2001: Impacts, Adaptation, and Vulnerability: Contributions of Working Group II to the Third Assessment of the IPCC* (Cambridge Univ. Press, Cambridge, 2001).
6. K. E. Trenberth et al., *J. Geophys. Res.* **103**, 14291 (1998).
7. C. F. Ropelewski, M. S. Halpert, *Mon. Weather Rev.* **115**, 1606 (1987).
8. _____, *J. Clim.* **2**, 268 (1989).
9. G. N. Kiladis, H. F. Diaz, *J. Clim.* **2**, 1069 (1989).
10. J. E. Cole, J. T. Overpeck, E. R. Cook, *Geophys. Res. Lett.*, in press.
11. M. Barlow, H. Cullen, B. Lyon, *J. Clim.* **15**, 697 (2002).
12. D. W. J. Thompson, J. M. Wallace, *Geophys. Res. Lett.* **25**, 1297 (1998).
13. G. Branstator, *J. Clim.* **15**, 1893 (2002).
14. The variability of 4-year–averaged, consecutive June–May periods was calculated based on monthly SSTs from 1948 to 1998. Fifty-one overlapping 4-year periods were used to calculate the standard deviation of 4-year averages, and this result was used to standardize the June 1998–May 2002 SST anomaly.
15. The model data are from a 24-member ensemble of the European Centre–Hamburg model (ECHAM4.5) run at the International Research Institute for Climate Prediction (IRI), an 18-member ensemble of the National Center for Environmental Predictions (NCEP) climate model, and a 9-member ensemble of the NASA Seasonal to Interannual Prediction Program (NSIPP) model. The configuration of the NCEP and ECHAM models uses triangular wavenumber 42 (T42) horizontal spectral resolution with 18 unequally spaced vertical (sigma) levels. The NSIPP model is a grid-point model with 2° horizontal resolution and 34 vertical levels. Observed, monthly SSTs are assigned to the mid-month date and are updated with linear interpolation for every time step at each ocean grid point. As of 2002, each of these model versions was being used by the three centers to make dynamical seasonal climate predictions.
16. Ensemble experiments are performed to detect the climate signal related to the imposed lower boundary forcing. In this approach, individual model realizations are begun from different atmospheric initial conditions, but each realization is subjected to identically evolving sea surface boundary conditions. The process of averaging the separate realizations extracts the recurrent atmospheric signal related to the boundary forcing and suppresses the random atmospheric fluctuations that are unrelated to that forcing.
17. M. Hoerling, A. Kumar, data not shown.
18. The experiments using an idealization of the 1998–2002 tropical SST forcing were performed with a recent version of the NCAR Community Climate Model known as CCM3. The standard model configuration is T42 horizontal spectral resolution with 18 unequally spaced vertical (hybrid) levels.
19. The spatial correlation of 200-mbar height anomalies poleward of 20°N between the GCM results forced by global SSTs and those calculated with the idealized 4-year–averaged tropical SSTs is 0.9.
20. S. G. Philander, *El Niño, La Niña, and the Southern Oscillation* (Academic Press, New York, 1990).
21. V. Markgraf, H. F. Diaz, in *El Niño and the Southern Oscillation: Multiscale Variability and Global and Regional Impacts,* H. F. Diaz, V. Margraf, Eds. (Cambridge Univ. Press, Cambridge, 2000), pp. 465–488.
22. At least three prior instances during the 20th century can be found in which La Niña conditions spanned three consecutive years, most notably 1908–1910, 1954–1957, and 1973–1975. Over the United States, the period 1954–1957 was a particularly severe drought period, whereas the other two protracted La Niña periods were not widespread droughts.
23. B. Rajagopalan, U. Lall, M. Cane, *J. Clim.* **10**, 2351 (1997).
24. A. Timmermann, *J. Atmos. Sci.* **56**, 2313 (1999).
25. T. R. Knutson, T. L. Delworth, K. W. Dixon, R. J. Stouffer, *J. Geophys. Res.* **104**, 30981 (1999).
26. T. R. Knutson, S. Manabe, *J. Clim.* **11**, 2273 (1998).

27. Supported by NOAA's Office of Global Programs Regional Integrated Sciences and Assessments Program, the Climate Variability/Pacific Program, and the Climate Dynamics and Experimental Predictions Program. We thank L. Goddard of the IRI and M. Suarez of NASA, who provided the ECHAM and NSIPP model data, respectively, and G. Bates and T. Y. Xu for assisting with model experiments and analysis.

3 October 2002; accepted 16 December 2002

Energetic Radiation Produced During Rocket-Triggered Lightning

Joseph R. Dwyer,[1]* Martin A. Uman,[2] Hamid K. Rassoul,[1] Maher Al-Dayeh,[1] Lee Caraway,[1] Jason Jerauld,[2] Vladimir A. Rakov,[2] Douglas M. Jordan,[2] Keith J. Rambo,[2] Vincent Corbin,[1] Brian Wright[1]

Using a NaI(Tl) scintillation detector designed to operate in electrically noisy environments, we observed intense bursts of energetic radiation (≫10 kiloelectron volts) during the dart leader phase of rocket-triggered lightning, just before and possibly at the very start of 31 out of the 37 return strokes measured. The bursts had typical durations of less than 100 microseconds and deposited many tens of megaelectron volts into the detector. These results provide strong evidence that the production of runaway electrons is an important process during lightning.

Attempts to measure x-ray emission from lightning have been intermittently reported since 1925, when C. T. R Wilson (*1*) first proposed that the strong electric fields associated with thunderstorms could accelerate electrons to relativistic energies. However, these results have been generally inconclusive because of the sporadic nature of lightning and the electromagnet-